SOUND SPEED AND ATTENUATION PREDICTIONS USING THE CORRECTED BIOT MODEL FOR GAS-BEARING MARINE SEDIMENTS

Guangying Zheng[a,b], Chuanxiu Xu[a,b], You shao[a,b]

[a]Hangzhou Applied Acoustics Research Institute, No. 715, Pingfeng Road, Xihu District, 310023, Hangzhou, P.R. China
[b]Science and Technology on Sonar Laboratory, No. 715, Pingfeng Road, Xihu District, 310023, Hangzhou, P.R. China

Guangying Zheng, 276454158@qq.com

Abstract: *As is well known, a small volume of gas bubbles existing in a sediment can greatly change the sound speed and attenuation in marine sediment. In this work, to investigate the sound propagation in a gas-bearing marine sediment, we integrate the volume vibrations of bubbles in pore water into the continuity equation of pore-fluid filtration in porous medium based on Biot theory, so as to obtain the continuity equation of pore-fluid filtration with bubble pulsation. On this basis, according to the relationship between the instantaneous radius of bubble and the background pressure of the medium under the linear vibration of bubble, as well as the equations of motion of the fluid medium and porous medium, a new displacement vector wave equation of porous medium under the influence of bubble is derived, which establishes the model for the sound speed dispersion and attenuation prediction under the gas-bearing sediments. The acoustic properties of gas-bearing sediments show three distinct zones of frequency-dependent behavior in numerical analysis. For the insonifying frequency below the gas-bubble resonance frequency, the phase velocity is lower, and the attenuation coefficient is significantly higher than that in non-gassy sediments. A transition zone near the resonance can be observed, in which the phase velocity rapidly increases. In particular, the phase velocity can highly exceed the non-gassy velocity at the resonance frequency. The attenuation is highest at frequencies close to the gas-bubble resonance frequency, which depends mainly on the bubble radius. Above the resonance, the phase velocity approaches a constant value similar to the non-gassy sediment, whereas the attenuation is higher than non-gassy attenuation and increases with the increasing frequency.*

Keywords: *gas-bearing marine sediment, sound speed, attenuation*

1. INTRODUCTION

It is well known that the presence of a small volume of gas bubbles in marine sediments can lead to a poor acoustic penetration[1]. And physical properties of gassy sediments are of interest to a number of offshore activities, including drilling operations and the siting of seafloor structures[2].

Three types[3,4] of gas bubbles in gassy sediments are generally considered as illustrated in Fig. 1(i.e., interstitial, reservoir, and sediment-displacing bubbles).

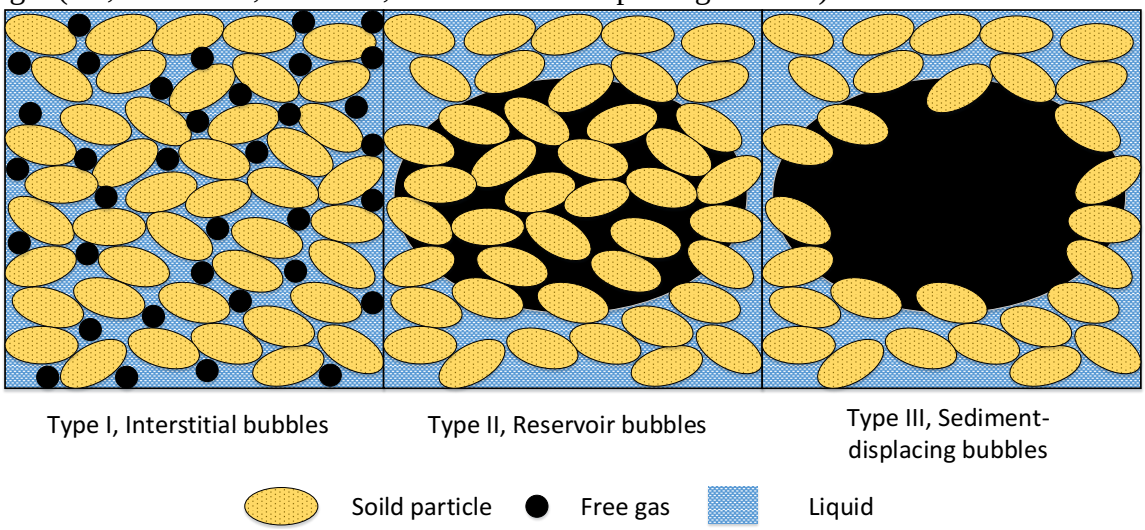

FIG. 1: Generic bubble classification for bubbles in sediments.

The most frequently used model for predicting acoustic scattering, sound speed and attenuation in gas-bearing marine sediments is proposed by Anderson and Hampton[5,6], The applicability of this model is limited to linear gas bubble pulsations, and leaves ambiguities for the inverse problem because of the plus/minus sign entering the expression of the complex sound speed. This sign ambiguity may result in the presence of both positive and negative bubble counts when inverting broadband acoustic data.

Recently, Zheng and Huang[7] developed a geoacoustic model to predict the acoustic response in gas-bearing sediments based on the Biot model and gas-bubble pulsations. This corrected model can be used to predict the sound speed and attenuation of the marine sediments of type I and type III, and can be used to estimate bubble size distributions through a full acoustic inversion. This paper reviews the method to predict the sound speed and attenuation using the corrected Biot model, and the acoustic response of these two type sediments is analysed.

2. MODELLING GAS-BEARING MARINE SEDIMENTS USING THE CORRECTED BIOT MODEL

2.1. Corrected Biot wave equation

The corrective poro-elastic equations derived by Zheng and Huang[7] are shown in Eqs. (1) and (2),

$$G_b\nabla^2\mathbf{u}+\left[H-G_b\right]\nabla\left(\nabla\cdot\mathbf{u}\right)-C\nabla\left(\nabla\cdot\mathbf{v}\right)-\beta C\nabla\beta_g=\frac{\partial^2}{\partial t^2}\left(\rho\mathbf{u}-\rho_w\mathbf{v}\right), \tag{1}$$

$$C\nabla\left(\nabla\cdot\mathbf{u}\right)-M\nabla\left(\nabla\cdot\mathbf{v}\right)-\beta M\nabla\beta_g=\frac{\partial^2}{\partial t^2}\left(\rho_w\mathbf{u}-\frac{\alpha\rho_w}{\beta}\mathbf{v}\right)-\frac{\eta F}{\kappa}\frac{\partial\mathbf{v}}{\partial t}, \tag{2}$$

where H, C and M denote the Biot elastic moduli, $\mathbf{u}$ denotes the absolute displacement vector of the solid framework, $\mathbf{v}$ denotes the relative displacement vector of the pore fluid relative to the solid framework, ρ is the density of the porous medium mixture, ρ_w is the density of pore fluid, η denotes the viscosity coefficient of the pore water, β is the porosity, κ denotes the permeability, α is the tortuosity, F denotes the high frequency complex correction factor, and β_g is the dynamic gas bubble void fraction.

Comparing these variables with the original Biot wave equation, two terms that involve $\nabla\beta_g$ have been introduced, which are again related to gas-bubble pulsations. In order to eliminate this gradient of the gas-bubble void fraction (i.e., $\nabla\beta_g$), the equation of motion of the effective fluid, which involves the effective sound pressure p_{eff} and the effective displacement $\mathbf{u}_{\text{eff}}=\mathbf{u}-\mathbf{v}$, is written as

$$-\nabla p_{\text{eff}}=\rho_{\text{eff}}\ddot{\mathbf{u}}_{\text{eff}}=\rho_{\text{eff}}\left(\ddot{\mathbf{u}}-\ddot{\mathbf{v}}\right), \tag{3}$$

where the effective density is

$$\rho_{\text{eff}}=\frac{\rho\tilde{\rho}_0-\rho_w^2}{\rho+\tilde{\rho}_0-2\rho_w}, \tag{4}$$

$$\tilde{\rho}_0=\frac{\alpha\rho_w}{\beta}-\frac{iF\eta}{\kappa\omega}. \tag{5}$$

The gas-bubble void fraction can be denoted as $\beta_g=4N\pi R^3/3$ by using N to denote the bubble number per unit volume. The relationship between the instantaneous radius of bubbles R and the effective perturbation pressure p_{eff} under the linear vibration of bubbles is given in, and ignoring higher-order perturbations:

$$\nabla\beta_g=-\frac{4\pi NR_0}{\rho\left(\omega_0^2-\omega^2+2ib_{\text{tot}}\omega\right)}\nabla p_{\text{eff}}, \tag{6}$$

where ω_0 and b_{tot} are the bubble resonance frequency and damping term, respectively, for type I gas-bearing sediments, air-bubble pulsations in pore water, which are given by Commander[8],

$$\omega_0^2=\left[\text{Re}\,\phi-2\sigma/\left(aP_{in,0}\right)\right]P_{in,0}/\rho_w a^2, \tag{7}$$

$$b_{\text{tot}}=2\eta/\left(\rho_w a^2\right)+\omega^2 a/\left(2c\right)+\text{Im}\left(P_{in,0}\phi\right)/\left(2\omega\rho_w a^2\right), \tag{8}$$

On the other hand, for type III gas-bearing sediments, air-bubble pulsations in saturated sediments, which are given by Yang and Church[9], the resonance frequency of gas bubble pulsations in a viscoelastic medium,

$$\omega_0^2=\left(3p_{g0}\,\text{Re}\left(\phi\right)-\frac{2\sigma}{R_0}+4G_0\right)\Big/\left(\rho_0R_0^2+\frac{4\eta_0R_0}{c_0}\right). \tag{9}$$

The damping term b_{tot}, which is sum of the viscous damping, thermal damping, radiation damping, interfacial damping and elastic damping. These damping terms are denoted as follows:

$$b_{\text{tot}} = b_{\text{vis}} + b_{\text{P-th}} + b_{\text{rad}} + b_{\text{int}} + b_{\text{el}}, \tag{10}$$

$$b_{\text{vis}} = 2\eta_0 \Big/ \left(\rho_0 R_0^2 + \frac{4\eta_0 R_0}{c_0} \right), \tag{11}$$

$$b_{\text{P-th}} = \left(\frac{3p_{g_0}\,\text{Im}(\phi)}{2\omega} \right) \Big/ \left(\rho_0 R_0^2 + \frac{4\eta_0 R_0}{c_0} \right), \tag{12}$$

$$b_{\text{rad}} = \left(\frac{\rho_0 \omega^2 R_0^3}{2c_0} \right) \Big/ \left(\rho_0 R_0^2 + \frac{4\eta_0 R_0}{c_0} \right), \tag{13}$$

$$b_{\text{int}} = -\sigma \Big/ \left(\rho_0 c_0 R_0^2 + 4\eta_0 R_0 \right), \tag{14}$$

$$b_{\text{el}} = 2G_s \Big/ \left(\rho_0 c_0 R_0 + 4\eta_0 R_0 \right), \tag{15}$$

where the complex polytropic function ϕ is denoted as follows:

$$\phi = 3\gamma_g \Big/ 1 - 3\left(\gamma_g - 1\right) \text{i}\chi \left[\left(\text{i}/\chi \right)^{1/2} \coth\left(\text{i}/\chi \right)^{1/2} - 1 \right], \tag{16}$$

where σ is Surface tension, $\chi = D/\omega R_0^2$, D is the thermal diffusivity of gas, and γ_g denotes the ratio of specific heats.

Substituting Eqs. (3) and (6) into Eqs. (1) and (2), the following equations are obtained,

$$G_b \nabla^2 \mathbf{u} + \left[H - G_b \right] \nabla \left(\nabla \cdot \mathbf{u} \right) - C \nabla \left(\nabla \cdot \mathbf{v} \right) = \frac{\partial^2}{\partial t^2} \left(\left(\rho + \gamma\tilde{\rho} \right) \mathbf{u} - \left(\rho_w + \gamma\tilde{\rho} \right) \mathbf{v} \right), \tag{17}$$

$$C \nabla \left(\nabla \cdot \mathbf{u} \right) - M \nabla \left(\nabla \cdot \mathbf{v} \right) = \frac{\partial^2}{\partial t^2} \left(\left(\tilde{\rho} + \rho_w \right) \mathbf{u} - \frac{\alpha \left(\rho_w + \tilde{\rho} \right)}{\beta} \mathbf{v} \right) - \frac{\eta F}{\kappa} \frac{\partial \mathbf{v}}{\partial t}, \tag{18}$$

where $\tilde{\rho} = \dfrac{4\pi N R_0 M \beta}{\left(\omega_0^2 - \omega^2 + 2ib_{\text{tot}}\omega \right)} \dfrac{\rho_{\text{eff}}}{\rho}$, $\gamma = 1 - \dfrac{K_w}{K_s}$.

Eqs. (17) and (18) can be written in another form:

$$\frac{G_b}{\text{ratio}_2} \nabla^2 \mathbf{u} + \frac{\left[H - G_b \right]}{\text{ratio}_2} \nabla \left(\nabla \cdot \mathbf{u} \right) - \frac{C}{\text{ratio}_2} \nabla \left(\nabla \cdot \mathbf{v} \right) = \frac{\partial^2}{\partial t^2} \left(\frac{\left(\rho + \gamma\tilde{\rho} \right)}{\left(\rho_w + \gamma\tilde{\rho} \right)} \rho_w \mathbf{u} - \rho_w \mathbf{v} \right), \tag{19}$$

$$\frac{C}{\text{ratio}_1} \nabla \left(\nabla \cdot \mathbf{u} \right) - \frac{M}{\text{ratio}_1} \nabla \left(\nabla \cdot \mathbf{v} \right) = \frac{\partial^2}{\partial t^2} \left(\rho_w \mathbf{u} - \frac{\alpha \rho_w}{\beta} \mathbf{v} \right) - \frac{\eta F}{\text{ratio}_1 \kappa} \frac{\partial \mathbf{v}}{\partial t}, \tag{20}$$

where $\text{ratio}_1 = \left(\rho_w + \tilde{\rho} \right) / \rho_w$ and $\text{ratio}_2 = \left(\rho_w + \gamma\tilde{\rho} \right) / \rho_w$.

It should be noted that ratio_1 and ratio_2 are both complex, with the moduli larger than 1, as long as the bubble volume fraction is not zero. Eqs. (19) and (20), show that the bubble volume vibration can be seen to alter the fluid compressibility, which leads to a decrease in the effective elastic modulus of the porous medium. Although the effective density of the porous medium is effectively unchanged by the presence of extremely small bubbles, there is a significant decrease in the speed of sound in the medium. Moreover, additional dissipation mechanisms are involved in the imaginary part of $\tilde{\rho}$ in Eqs. (17) and (18), which are due to the radiation, interfacial, viscous, thermal, and elastic damping of the pulsating air bubbles.

Note that if $\beta_g = 0$, there are no bubbles in the porous medium; the bubble number per unit volume is $N = 0$. In that case, Eqs. (17) and(18) become identical to the Biot equations. Thus, the present theory is tantamount to Biot theory when the gas-bubble pulsation is unaccounted for.

3. RESULTS

3.1. Acoustic response of type I gas-bearing sediments

	parameters	values	parameters	values
Biot model parameters	Grain diameter	0.128mm/0.781mm	Fluid viscosity	1.002×10^{-3}Pa·s
	Grain density	2517 kg/m^3	porosity	0.439
	Grain bulk modulus	5.1×10^{10} Pa	permeability	2.54×10^{-10} m^2
	Fluid density	999 kg/m^3	Pore size	1.53×10^{-4} m
	Fluid bulk modulus	2.193×10^{9} Pa	Structure factor	1.35
	Frame bulk modulus	5.31×10^{7} Pa	Frame shear modulus	5.58×10^{6} Pa
	Longitudinal logarithmic decrement	0.15	Shear logarithmic decrement	0.15
Gas bubble parameters	Gas density	1.1691 kg/m^3	Thermal diffusivity	2.4×10^{-5} m^2/s
	Gas velocity	340 m/s	Surface tension	72.75×10^{3} N/m
	Equilibrium pressure	1.01×10^{5} Pa	ratio of specific heat	1.4

Table 1: Model input parameters for gas-bearing sediments.

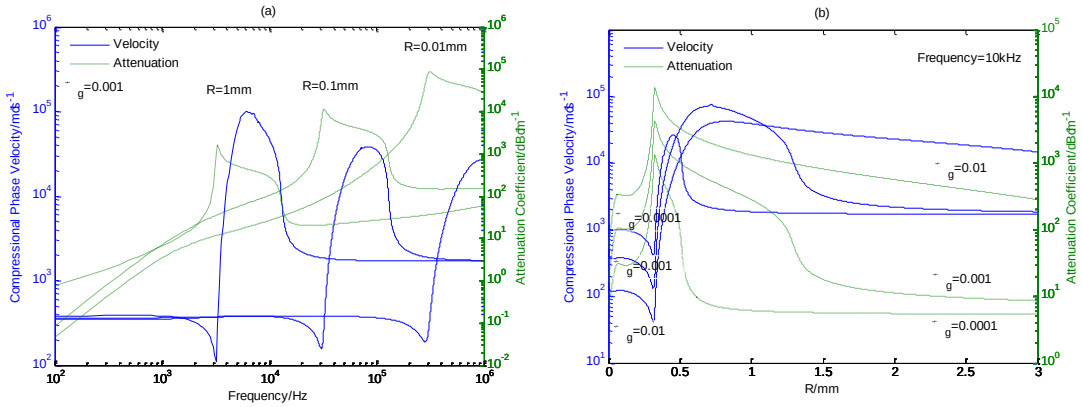

Fig. 2: Acoustic response of gas-bearing sediments according to the model in this paper. (a) Variation in acoustic velocity and attenuation coefficient with frequency for a range of gas bubble sizes(constant gas content 0.001) and (b) Variation in acoustic velocity and attenuation coefficient with bubble radius for a range of gas contents(constant excitation frequency of 10kHz).

A typical set of response curves in Fig. 2 shows three distinct zones of frequency-dependent behavior. These model input parameters in Table 1 were measured from sediment samples in our experiment, and a delta-function bubble size distribution is provided. For frequencies below resonance, the velocity is significantly reduced and the attenuation is higher than that in gas-free sediments. Near resonance, a transition zone is seen, where phase velocity dramatically increases. At resonance, the gassy sediment is highly dispersive and the velocity can greatly exceed the gas-free velocity, which has not been measured in field data. Attenuation is highest at a frequency near the bubble resonance frequency, which is primarily dependent on the radius of the bubble. Above the resonance frequency, the bubbles scatter the sound and the acoustic response essentially that of the surrounding medium, so the velocity remains constant at a value commensurate with the gas-free sediment, while the attenuation is higher than in gas-free sediment and increases with frequency. Note that the attenuation coefficient calculated here is related to acoustical bubble scattering(which also includes terms for fluid viscous damping at the bubble walls, bubble radiation damping and bubble gas

thermal damping) and the dissipation due to the relative motion between pore fluid and framework.

3.2. Acoustic response of type III gas-bearing sediments

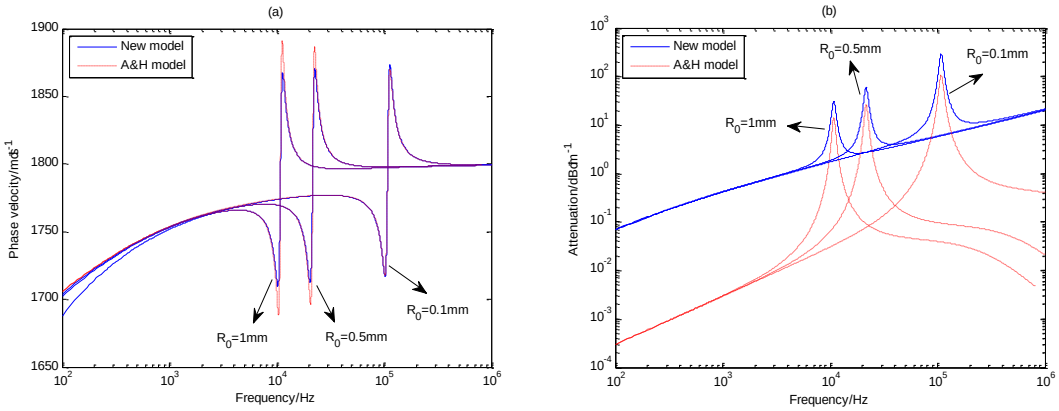

FIG. 3: (a) Sound speed and (b) attenuation as frequency functions for a series of mono-dispersed bubble populations, which all have a void fraction of 10^{-5} (i.e., the radius for each bubble labeled in the figure). The solid line denotes the results calculated by the proposed model, whereas the dashed line denotes the results of the A&H model.

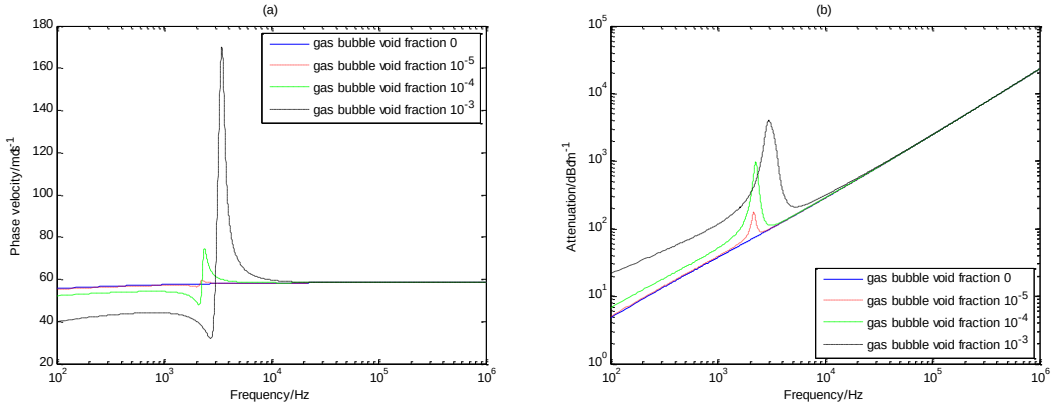

FIG. 4: Variation in the (a) shear wave phase velocity and (b) attenuation coefficient with frequency for a range of gas contents (constant gas-bubble radius of 5 mm).

Fig. 3 shows a comparison of the sound speed and attenuation for the fast wave between the proposed model and the A&H model. Notably, significant differences between the predictions of these two models are shown in Fig.3b. The current model predicts higher attenuation than the results predicted by the A&H model. The main reason for this scenario is that the current model involves more dissipation regimes: the relative motion between the pore water and solid frame, elastic damping, and interface damping. The main advantage of the current model is that its expression that predicts the velocity does not contain sign ambiguity and can be applied to an inversion model, which requires simultaneous information on sound speed and attenuation data.

What's more, the current model can be used to predict the phase velocity and attenuation coefficient of a shear wave(Fig. 4).The shear wave response curves show similar frequency-dependent behavior to that of a fast wave. The phase velocity is lower than that in gas-free sediments because the insonifying frequency is lower than the resonance frequency of the bubbles. The phase velocity at the resonance can significantly exceed the non-gassy velocity, and attenuation is the highest.

4. CONCLUSIONS

This study presents the corrected Biot model for gas-bearing marine sediments. This model can be used to predict the sound speed and attenuation of longitudinal and shear waves in the presence of linear bubble pulsations in gassy marine sediments. Numerical results for the phase velocity and attenuation coefficient show similar frequency dependencies for type I and type III sediments, longitudinal and shear waves. By contrast, the results for the attenuation of fast waves show a significant difference due to the additional damping regimes comparing to the A&H model. The current model has three major advantages: 1) this current model is applicable to the two type of marine sediments; 2) It can predict sound speeds, attenuation coefficients, and reflection coefficients for fast, slow, and shear waves; 3) It can also be utilized in inversion models that require simultaneous data on sound speed and attenuation.

5. ACKNOWLEDGEMENTS

This work was supported by the National Natural Science Foundation of China (Grant No. 61471327). This work was funded by the National Defense Science and Technology Innovation Zone.

REFERENCES

[1] **P. Fleischer, T. Orsi, M. Richardson, and A. Anderson**, Distribution of free gas in marine sediments: a global overview, *GeoMarine Letters*, volume 21, pp. 103–122, 2001.
[2] **G. C. Sills and S. J. Wheeler**, The significance of gas for offshore operations, *Continental Shelf Research*, volume 12, pp. 1239-1250, 1992.
[3] **G. B. N. Robb, T. G. Leighton, J. K. Dix, A. I. Best, V. F. Humphrey and P. R. White**, Measuring bubble populations in gassy marine sediments: a review, Futures in Acoustics: Today's Research-Tomorrow's Careers. *Proceedings of the Institute of Acoustics Spring Conference*, volume 28, pp. 60–68, 2006.
[4] **A. L. Anderson, F. Abegg, J. A. Hawkins, M. E. Duncan and A. P. Lyons**, Bubble populations and acoustic interaction with the gassy floor of Eckernförde bay, *Continental Shelf Research*, volume 18, pp. 1807–1838, 1998.
[5] **A. L. Anderson and L. D. Hampton**, Acoustics of gas-bearing sediments. I. Background, *Journal of the Acoustical Society of America*, volume 67, pp. 1865–1889, 1980.
[6] **A. L. Anderson and L. D. Hampton**, Acoustics of gas-bearing sediment. II. Measurements and models," *Journal of the Acoustical Society of America*, volume 67, pp. 1890–1903, 1980.
[7] **G. Y. Zheng and Y. W. Huang**, Effect of linear bubble vibration on wave propagation in unsaturated porous medium containing air bubbles, *Acta Physica. Sinica*, volume, 65, pp. 234301, 2016.
[8] **K. W. Commander and A. Prosperetti**, Linear pressure waves in bubbly liquids: Comparison between theory and experiment, *Journal of the Acoustical Society of America*, volume 85, pp. 732–746, 1989.
[9] **X. Yang and C. C. Church**, A model for dynamics of gas bubbles in soft tissue, *Journal of the Acoustical Society of America*, volume 118, pp. 3595–3606, 2005.